Research Article

Molecular Cancer Therapeutics

Distinct Roles of Cytochrome *P*450 Reductase in Mitomycin c Redox Cycling and Cytotoxicity

Yun Wang[1], Joshua P. Gray[3], Vladimir Mishin[2], Diane E. Heck[4], Debra L. Laskin[2], and Jeffrey D. Laskin[1]

Abstract

Mitomycin c (MMC), a quinone-containing anticancer drug, is known to redox cycle and generate reactive oxygen species. A key enzyme mediating MMC redox cycling is cytochrome *P*450 reductase, a microsomal NADPH-dependent flavoenzyme. In the present studies, Chinese hamster ovary (CHO) cells overexpressing this enzyme (CHO-OR cells) and corresponding control cells (CHO-WT cells) were used to investigate the role of cytochrome *P*450 reductase in the actions of MMC. In lysates from both cell types, MMC was found to redox cycle and generate H_2O_2; this activity was greater in CHO-OR cells (V_{max} = 1.2 ± 0.1 nmol H_2O_2/min/mg protein in CHO-WT cells versus 32.4 ± 3.9 nmol H_2O_2/min/mg protein in CHO-OR cells). MMC was also more effective in generating superoxide anion and hydroxyl radicals in CHO-OR cells, relative to CHO-WT cells. Despite these differences in MMC redox cycling, MMC-induced cytotoxicity, as measured by growth inhibition, was similar in the two cell types (IC_{50} = 72 ± 20 nmol/L for CHO-WT and 75 ± 23 nmol/L for CHO-OR cells), as was its ability to induce G_2-M and S phase arrest. Additionally, in nine different tumor cell lines, although a strong correlation was observed between MMC-induced H_2O_2 generation and cytochrome *P*450 reductase activity, there was no relationship between redox cycling and cytotoxicity. Hypoxia, which stabilizes MMC radicals generated by redox cycling, also had no effect on the sensitivity of tumor cells to MMC-induced cytotoxicity. These data indicate that NADPH cytochrome *P*450 reductase–mediated MMC redox cycling is not involved in the cytotoxicity of this chemotherapeutic agent. *Mol Cancer Ther; 9(6); 1852–63. ©2010 AACR.*

Introduction

Mitomycin c (MMC) is a quinone-containing alkylating agent widely used for the treatment of solid tumors (1). It has been postulated that bioreductive activation of MMC is responsible for its antitumor and cytotoxic properties. In this reaction, a one- or two-electron enzymatic reduction of the quinone moiety in MMC generates a semiquinone free radical intermediate or a hydroquinone intermediate, respectively, both of which are potent DNA-alkylating agents (2, 3). Under aerobic conditions, the semiquinone intermediate is oxidized back to the parent compound generating superoxide anion (see Fig. 1A for the structure of MMC and redox cycling pathway). Superoxide anion then dismutates to H_2O_2; in the presence of trace metals, H_2O_2 forms hydroxyl radicals (4). These reactive oxygen species (ROS) can damage intracellular macromolecules including lipids, protein, and DNA, resulting in oxidative stress and toxicity. Under hypoxic conditions, redox cycling is limited and the MMC semiquinone rearranges to form a DNA-reactive hydroquinone intermediate (5–7).

Several different flavoenzymes have been shown to catalyze the one electron reduction of MMC including NADPH-cytochrome *P*450 reductase (EC 1.6.2.4), NADH-cytochrome b5 reductase, xanthine oxidase, and nitric oxide synthase, and it has been suggested that these enzymes are mediators of MMC-induced cytotoxicity (8–12). For example, Belcourt and colleagues (13) have shown that overexpression of cytochrome *P*450 reductase in Chinese hamster ovary (CHO) cells enhances their sensitivity to MMC under both oxygenated and hypoxic conditions. Increased sensitivity to MMC under these conditions has also been described in CHO cells engineered to express nuclear cytochrome *P*450 reductase (14). Similarly, viral delivery of cytochrome *P*450 reductase increases the sensitivity of human breast cancer cells to MMC, although this is only evident under oxygenated conditions (15). Martinez and colleagues (16) also reported increased sensitivity of human MDA 231 breast carcinoma cells overexpressing cytochrome *P*450 reductase to MMC. In contrast, Fitzsimmons and colleagues (17) found that there was no direct correlation between sensitivity to MMC and levels of cytochrome *P*450

Authors' Affiliations: [1]Environmental and Occupational Medicine, UMDNJ-Robert Wood Johnson Medical School and [2]Pharmacology and Toxicology, Rutgers University, Piscataway, New Jersey; [3]Science, US Coast Guard Academy, New London, Connecticut; and [4]Environmental Health Science, New York Medical College, Valhalla, New York

Corresponding Author: Jeffrey D. Laskin, Department of Environmental and Occupational Medicine, UMDNJ-Robert Wood Johnson Medical School, 170 Frelinghuysen Road, Piscataway, NJ 08854. Phone: 732-445-0170; Fax: 732-445-0119. E-mail: jlaskin@eohsi.rutgers.edu

doi: 10.1158/1535-7163.MCT-09-1098

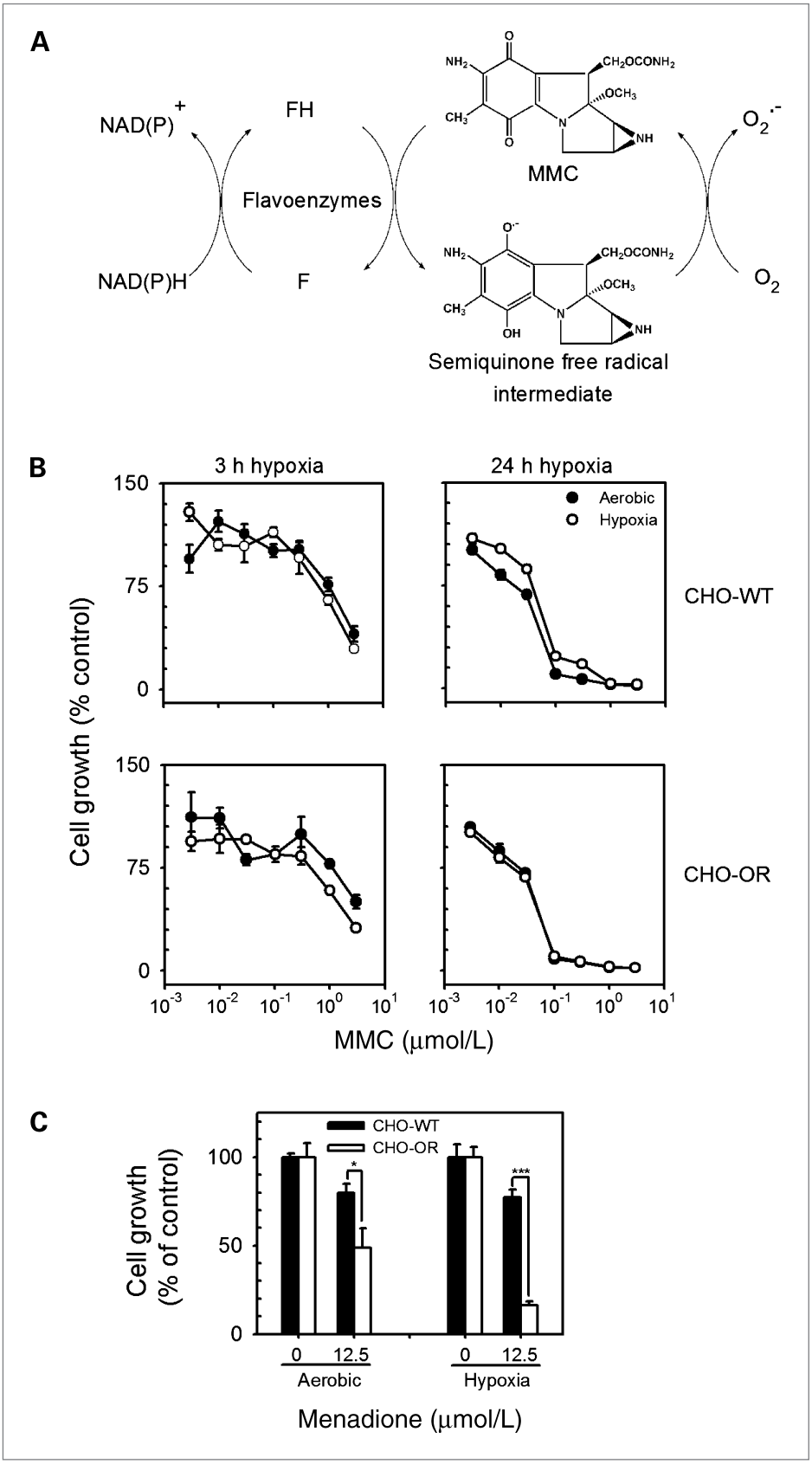

Figure 1. Redox cycling and growth-inhibitory activity of MMC. A, MMC undergoes a one-electron reduction to form a semiquinone free radical intermediate during redox cycling. In the presence of molecular oxygen, the radical disproportionates to form superoxide anion and the parent compound. Modified from Bachur et al. (8). B, comparison of the cytotoxicity of MMC under aerobic and hypoxic conditions in CHO cells. CHO-WT cells and CHO-OR cells were seeded into 6- or 24-well culture plates (2.5×10^4 cells/well or 5,000 cells/well) and allowed to adhere overnight. The medium was then replaced with growth medium supplemented with increasing concentrations of MMC and cultured either 3 h (left, 3-h exposure to MMC) or 24 h (right, 4-d exposure to MMC) under aerobic or hypoxic conditions as described in Materials and Methods. Cell growth was assayed after an additional 3 d in culture by counting cells using a Coulter Counter. Points, mean ($n = 3$); bars, SEM. C, cytotoxicity of menadione under aerobic and hypoxic conditions in CHO cells. *, $P < 0.05$; ***, $P < 0.001$.

reductase across 69 cell lines obtained from the National Cancer Institute (NCI) Tumor Cell line panel. Findings in these studies that sensitivity to MMC correlated with DT-diaphorase, an obligate two-electron reductase, suggested that the MMC-derived hydroquinone intermediate is more likely to mediate its antitumor activity.

The present studies were designed to further explore the role of cytochrome *P*450 reductase in the cytotoxicity of MMC under oxygenated and hypoxic conditions. For these studies, we compared MMC-induced cytotoxicity and redox cycling in cell lines varying in cytochrome *P*450 reductase activity including CHO cells constructed to overexpress the enzyme. Our results show that neither redox cycling nor stabilization of the MMC radical by hypoxia is correlated with the cytotoxicity of MMC. These data provide further support for the concept that microsomal cytochrome *P*450 reductase plays a limited role in mediating the antitumor activity of MMC.

Materials and Methods

Chemicals and reagents

cDNA-expressed NADPH cytochrome *P*450 reductase from microsomal fractions of insect cells (Supersomes) was obtained from BD Gentest. 10-Acetyl-3, 7-dihydroxyphenoxazine (Amplex Red) and 2',7'-dichlorofluorescein diacetate (DCFH-DA) were from Molecular Probes. Mouse monoclonal antibody to cytochrome *P*450 reductase was obtained from Santa Cruz. MMC, NADPH, catalase, and all other chemicals were from Sigma.

Cells and treatments

Cytochrome *P*450 reductase–overexpressing CHO cells (CHO-OR) and control cells expressing empty vector (CHO-WT) were kindly provided by Dr. Jun Yan Hong at the University of Medicine and Dentistry of New Jersey (Piscataway, NJ). CHO-OR cells have been reported to express 30-fold more cytochrome *P*450 reductase relative to CHO-WT cells (18). We measured cytochrome *P*450 reductase activity in lysates of the cells using a cytochrome *c* reductase assay kit (Sigma-Aldrich), and found that CHO-WT cells contained 2.4 units of cytochrome *P*450 reductase activity per milligram of protein and CHO-OR cells contained 83.7 units of cytochrome *P*450 reductase activity per milligram of protein, in which one unit reduces 1 nmol/L of oxidized cytochrome *c* in the presence of 100 μmol/L NADPH per minute at pH 7.8 at 25°C. Overexpression of the enzyme was confirmed by Western blotting using antibody to cytochrome *P*450 reductase (data not shown). Murine lung epithelial cells (MLE 15 cells) were obtained from Dr. Jacob N. Finkelstein (University of Rochester, Rochester, NY). All other cell lines were from the American Type Culture Collection. Stocks of cells were maintained in liquid nitrogen and used fewer than 6 months after resuscitation. Cell lines were not further tested or authenticated. CHO-WT, CHO-OR, and PC-3 cells were maintained in Ham's F12K medium. MLE 15, RAW 264.7, C2, S-180, B16, HL-60, HT-29, and HeLa cells were maintained in DMEM. All medium was supplemented with 10% fetal bovine serum, penicillin (100 U/mL), and streptomycin (100 μg/mL). For CHO cells, the growth medium was also supplemented with 500 μg/mL hygromycin B (Invitrogen). Cells were cultured at 37°C in 5% CO_2 in a humidified incubator. Tissue culture reagents were from Life Technologies Bethesda Research Laboratories.

Cell growth inhibition was evaluated as previously described (19). Briefly, cells were plated at low density (2.5–10×10^4 cells/well) in six-well tissue culture dishes and allowed to adhere overnight. The medium was then replaced with growth medium supplemented with increasing concentrations of MMC. To induce hypoxia, the cells were placed in an MIC-101 Modular Incubator Chamber (Billups-Rothenberg, Inc.), flushed with 95% N_2/5% CO_2 twice, and then incubated at 37°C for 24 hours. After an additional 3 to 5 days in culture, the cells were removed from the dishes with trypsin and counted using a Z1 Coulter Particle Counter (Beckman Coulter). Concentrations of MMC that caused 50% growth inhibition (IC_{50}) were then determined. In some experiments, hypoxia was induced using a two-enzyme system (glucose oxidase and catalase) as previously described (20), with some modifications. Briefly, cells were plated in 24-well tissue culture plates (5,000 cells/well) and allowed to adhere overnight. The medium was then replaced with 2 mL growth medium supplemented with 10 mmol/L glucose with or without 2 U/mL glucose oxidase and 120 U/mL catalase. After 10 minutes, MMC was added and cells were incubated at 37°C for 3 hours. Cells were then washed and refed with fresh growth medium. After an additional 3 days at 37°C, cells were trypsinized and counted as described above. Depletion of oxygen by the two-enzyme system was confirmed in an Oxygraph with a Clark-type electrode (Yellow Springs Instruments). Earlier studies have suggested that, under hypoxic conditions, cell culture plasticware, but not glassware, can release trace amount of oxygen that can mediate redox cycling (21, 22). We found that there were no significant differences in the effects of MMC on cell growth under normoxic or hypoxic conditions when either plastic or glass culture dishes were used. Thus, using the Modular Incubator Chamber with CHO-OR cells on plastic dishes, the IC_{50} for MMC was 75 and 78 nmol/L under normoxic and hypoxic conditions, respectively, whereas the IC_{50} for MMC was 75 and 80 nmol/L, respectively, for glass dishes. Using the two-enzyme hypoxia system with CHO-OR cells, for plastic dishes, the IC_{50} for MMC was 3.0 and 2.0 μmol/L under normoxic and hypoxic conditions, respectively, whereas the IC_{50} for MMC was 2.5 and 2.0 μmol/L, respectively, for glass dishes.

To prepare lysates, cells were scraped from culture dishes in PBS, washed, and centrifuged ($800 \times g$, 5 min). Cell pellets were stored at −70°C until analysis. Before enzyme assays, cell pellets were resuspended in PBS ($\sim 1 \times 10^7$ cells/0.5 mL) and sonicated on ice using a sonic dismembrator (ARTEK Systems, Inc.). Homogenates

Table 1. MMC-induced growth inhibition and kinetics parameters of MMC-stimulated hydrogen peroxide generation in lysates of different cell types

Species	Cell type	Origin	IC_{50} (nmol/L)*		Kinetics parameters	
			Aerobic	Hypoxic	K_m (μmol/L)†	V_{max} (nmol H_2O_2/min/mg protein)
Hamster	CHO-WT	Ovary	72 ± 20	85 ± 15	117 ± 20	1.2 ± 0.1
	CHO-OR	Ovary	75 ± 23	78 ± 26	292 ± 80	32.4 ± 3.9
Mouse	MLE 15	Lung	40 ± 26	35 ± 22	481 ± 28	8.2 ± 0.2
	RAW 264.7	Macrophage	73 ± 12	67 ± 6	381 ± 58	5.0 ± 0.7
	C2	Muscle	40 ± 28	50 ± 42	235 ± 46	1.9 ± 0.0
	S 180	Sarcoma	67 ± 15	60 ± 10	255 ± 65	2.8 ± 0.1
	B16	Melanoma	78 ± 13	63 ± 6	240 ± 17	3.1 ± 0.1
Human	HL-60	Leukemia	50 ± 26	50 ± 26	126 ± 9	1.2 ± 0.1
	HT-29	Colon	77 ± 12	70 ± 17	225 ± 35	3.9 ± 0.2
	HeLa	Cervix	68 ± 28	73 ± 46	242 ± 9	3.3 ± 0.2
	PC-3	Prostate	35 ± 30	40 ± 24	124 ± 13	1.1 ± 0.1

NOTE: Each point represents the mean of three independent determinations ± SEM.

*IC_{50}, concentration of MMC inhibiting cell growth by 50%. Cells were exposed to either aerobic or hypoxic conditions for 24 h using a modular incubator chamber as described in Materials and Methods. IC_{50}s for each cell type obtained under aerobic and hypoxic conditions were not significantly different ($P \geq 0.1$).

†Using increasing concentrations of MMC, reaction rates were measured in the linear phase in standard reaction mixes in the presence of NADPH (0.5 mmol/L). K_m and V_{max} values were obtained using the Michaelis-Menton kinetics.

were then sequentially centrifuged at 4°C (3,000 × *g* and 12,000 × *g*, for the removal of cellular debris and mitochondrial fractions, respectively). The resulting supernatant fractions were used in enzyme assays. Protein concentrations were quantified using the *Dc* protein assay kit (Bio-Rad) with bovine serum albumin as the standard.

Cell cycle analysis

Cell cycle analysis was done as previously described, with some modifications (23). Briefly, cells were seeded into six-well plates at 2.5×10^5 cells per well and allowed to adhere overnight. The medium was then replaced with growth medium supplemented without or with MMC. After 24 hours, cells were harvested, fixed in 70% ice-cold ethanol, and stored at −20°C until further processing. For DNA analysis, cells were treated with propidium iodide (10 μg/mL) and RNase (40 μg/mL) for 30 minutes and then analyzed on a Cytomics FC 500 flow cytometer (Beckman Coulter). Data were analyzed by the CXP software (Beckman Coulter).

MMC redox cycling assays

Redox cycling of MMC in lysates was quantified by the formation of H_2O_2, hydroxyl radicals, and superoxide anion. The Amplex Red/horseradish peroxidase method was used to assay hydrogen peroxide production (24). Briefly, assays were run at 37°C in standard reaction mixes in 100 μL potassium phosphate buffer (50 mmol/L, pH 7.8) containing 0 to 0.5 mmol/L NADPH, 0 to 0.5 mmol/L MMC, 25 μmol/L Amplex Red, 1 U/mL horseradish peroxidase, and 1.25 μg/mL cytochrome *P*450 reductase or 100 μg/mL of cell lysate protein. The fluorescent product resorufin was detected using an HTS 7000 Plus Bio Assay Reader (Perkin-Elmer Life Sciences) with 540 nm excitation and 595 nm emission filters. Increases in fluorescence intensity were measured every 2.5 minutes for 30 minutes. Fluorescence was converted into amount of H_2O_2 based on calibration standards.

The generation of 2-hydroxyterephthalate from terephthalate was used as an indicator of hydroxyl radical production (25). Standard reaction mixes in 0.2 mL potassium phosphate buffer (20 mmol/L, pH 7.4) contained 150 μg/mL cell protein from supernatant fractions, 1 mmol/L terephthalate, and 0.5 mmol/L NADPH. Reactions were initiated by the addition of Fe^{3+}/EDTA (100/110 μmol/L) to the assay mix. After incubation at 37°C for 1 hour, reactions were stopped by adding an equal volume of ice-cold methanol. 2-Hydroxyterephthalate was quantified by high-performance liquid chromatography with fluorescence detection as previously described (25). In these experiments, catalase (400 U/mL) was found to inhibit hydroxyl radical formation.

Superoxide anion was assayed by the formation of 2-hydroxyethidium from dihydroethidium (26). Standard reaction mixes described above were used except that Fe^{3+}/EDTA was omitted and dihydroethidium (40 μmol/L) was used in place of terephthalate. 2-Hydroxyethidium formation was detected using a Shimadzu HPLC fitted with a Luna C18 column (250 mm × 2.0 mm, Phenomenex) and a fluorescence detector with excitation and emission wavelengths set at 510 and 595 nm, respectively. The mobile phase consisted of a linear (10–40%) gradient of acetonitrile in 0.1% trifluoroacetic acid and was run at a flow rate of 0.2 mL/min for 45 minutes.

2-Hydroxyethidium eluted from the column with a retention time of 40 minutes.

Oxygen consumption was determined using a Clark-type electrode in a mix of 50 mmol/L potassium phosphate (pH 7.8), 0.5 mmol/L NADPH, 10 mmol/L glucose-6-phosphate, 0.5 U/mL glucose-6-phosphate dehydrogenase, 0.1 mg/mL of cell lysate protein, 0.5 mmol/L MMC in a final volume of 1.2 mL. At the end of the experiment, several grains of sodium dithionite were added to deplete remaining oxygen for calibration. In some experiments, an Oxygraph system was used to quantify the effects of MMC (0.5 mmol/L)

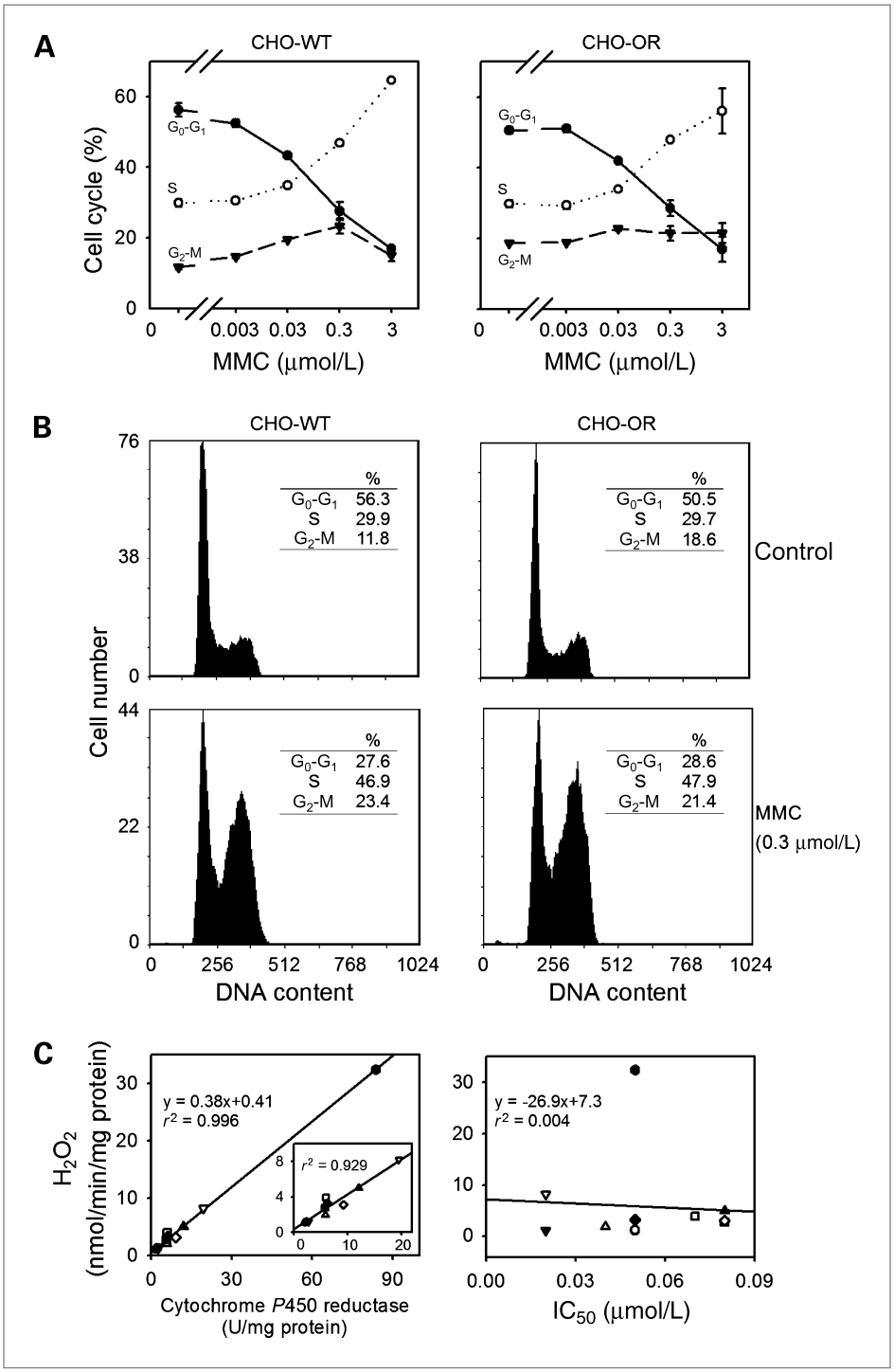

Figure 2. Cytotoxicity of MMC. A and B, effects of MMC on the cell cycle of CHO-WT and CHO-OR cells. Cell cycle analysis was done 24 h after treatment with MMC by flow cytometry after propidium iodide staining. A, analysis of cell cycle in CHO-WT and CHO-OR cells following treatment with increasing concentrations of MMC. B, DNA histograms of CHO cells with or without 0.3 μmol/L MMC treatment. One representative experiment is shown. DNA content is presented on a linear scale. C, comparison of cytochrome *P*450 reductase activity, MMC-induced redox cycling, and cytotoxicity in different tumor cell lines. Left, correlation between cellular cytochrome *P*450 reductase activity and MMC-induced H_2O_2 production. Cytochrome *P*450 reductase activity in the cell lines was quantified using a cytochrome *c* reduction assay and presented in an earlier publication (27). The V_{max} for MMC-induced H_2O_2 generation (Table 1) was used to compare MMC-induced redox cycling with cellular cytochrome *P*450 reductase activity. Inset, the correlation between cytochrome *P*450 reductase activity and MMC-induced H_2O_2 production when CHO-OR cells were not included in the analysis. Right, lack of correlation between MMC-induced redox cycling and cellular cytotoxicity. Redox cycling capacity of the cell lines was plotted against the concentration of MMC IC_{50} in each cell line (Table 1). ●, PC-3; ○, CHO-WT; ▼, HL-60; △, C2; ■, S-180; □, HT-29; ◆, HeLa; ◇, B16; ▲, RAW 264.7; ▽, MLE 15; ⬣, CHO-OR.

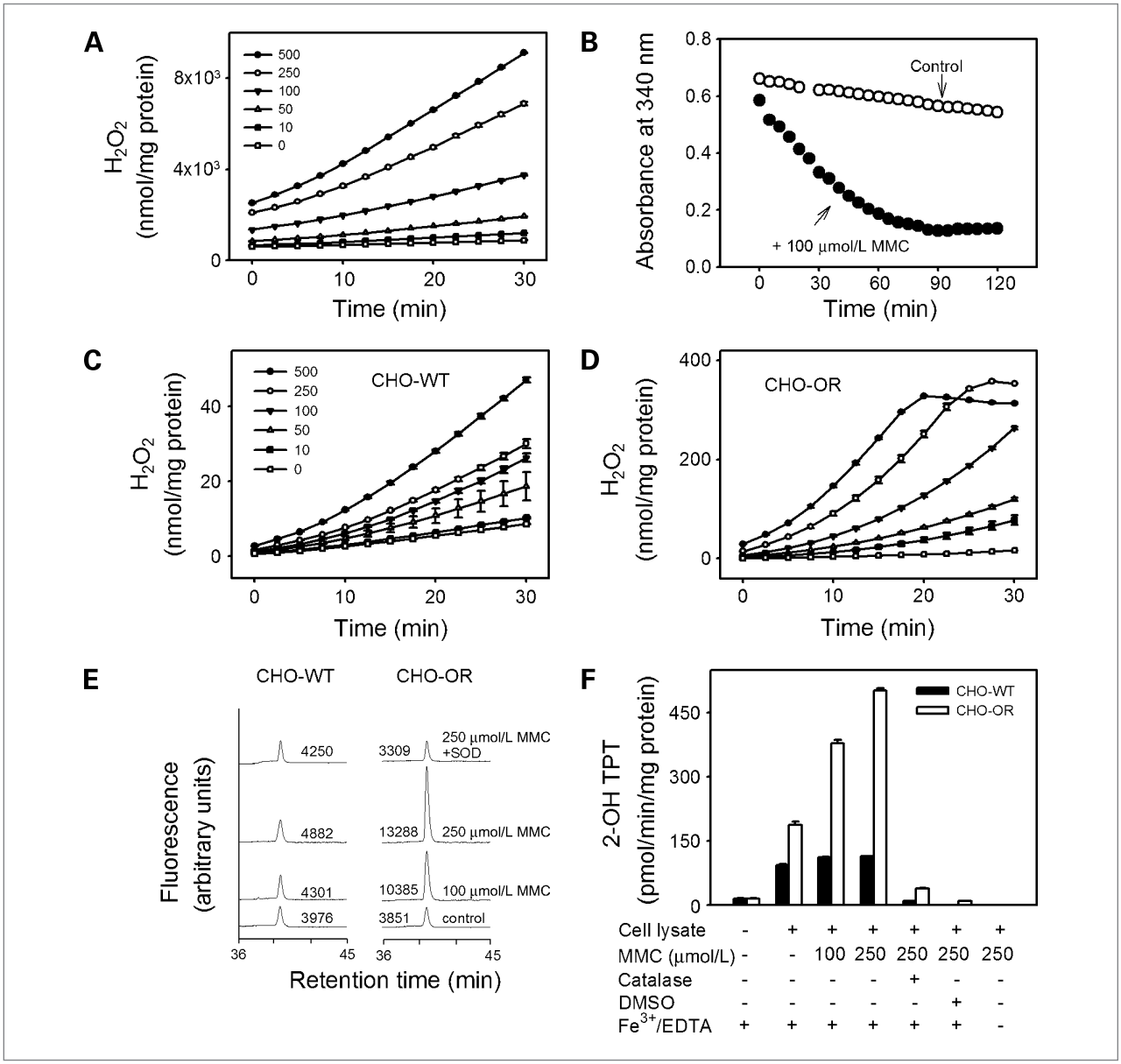

Figure 3. Redox cycling of MMC by recombinant cytochrome *P*450 reductase and lysates of CHO cells. A, ability of rat recombinant cytochrome *P*450 reductase to redox cycle MMC. H_2O_2 production was assayed in enzyme reactions run in the absence or presence of increasing concentrations of MMC using Amplex Red/horseradish peroxidase. Points, mean (n = 3); bars, SEM. B, metabolism of NADPH in reactions containing rat recombinant cytochrome *P*450 reductase. NADPH (100 μmol/L) in reaction mixes was assayed in the absence (○) or presence (●) of 100 μmol/L MMC. C and D, MMC-induced H_2O_2 generation during redox cycling. MMC-induced H_2O_2 production in lysates from CHO-WT cells (C) and CHO-OR cells (D) was assayed in absence or presence of increasing concentrations of MMC. Points, mean (n = 3); bars, SEM. E, generation of superoxide anion by MMC. Superoxide anion in enzyme assays was quantified by the formation of 2-hydroxyethidium from dihydroethidium as measured by high-performance liquid chromatography with fluorescence detection. In some assays, superoxide dismutase (350 U/mL) was added to inhibit the accumulation of superoxide anion. One representative experiment is shown. The numbers indicate the areas under each peak in arbitrary units. F, generation of hydroxyl radicals by MMC. Hydroxyl radicals in enzyme assays were quantified by the formation of 2-hydroxyterephthalate (2-OH TPT) from terephthalate. Columns, mean (n = 2); bars, SD. In some assays, catalase (400 U/mL) or DMSO (70 mmol/L) was added to inhibit hydroxyl radical formation or its reaction with terephthalate, respectively. Note that the formation of hydroxyl radicals was dependent on the presence of redox active iron. All reactions contained 0.5 mmol/L NADPH.

on oxygen consumption in intact cells (2.5×10^6/mL). Disappearance of NADPH in enzyme reactions was assayed in 1 mL spectrophotometer cuvettes by quantifying decreases in absorbance at 340 nm as previously described (27).

Measurement of ROS in intact cells

Intracellular ROS were quantified using DCFH-DA in conjunction with flow cytometry as previously described (28). In brief, cells were suspended in PBS (1×10^6/mL) and incubated with 5 μmol/L DCFH-DA at 37°C in a

shaking water bath. After 15 minutes, MMC was added. After an additional 3 hours, cellular fluorescence was analyzed by flow cytometry as described above.

Statistical analysis

Each determination was done in duplicate or triplicate, and repeated two or three times. Differences were analyzed for statistical significance using the one-way ANOVA or paired *t* test with GraphPad Instat software; $P < 0.05$ was considered significant. GraphPad software was also used to calculate enzyme kinetic parameters.

Results

Cytotoxicity of MMC

In initial studies, we examined the cytotoxicity of MMC using CHO-WT cells. MMC was found to effectively inhibit the growth of these cells after short (3 h) and long-term (4 d) exposure (Table 1; Fig. 1B); greater cytotoxicity was observed after long-term exposure. Growth inhibition by MMC was associated with the arrest of cells in the G_2-M and S phases of the cell cycle (Fig. 2A and B). Previous work suggested that MMC-induced cytotoxicity was due, at least in part, to redox cycling through cytochrome *P*450 reductase (8, 29). Using recombinant cytochrome *P*450 reductase, we found that MMC was readily able to redox cycle, generating superoxide anion and H_2O_2 in the process (data not shown; Fig. 3A). Redox cycling was time and MMC concentration dependent; the V_{max} for H_2O_2 production was 425.6 ± 34.6 nmol/min/mg protein and the apparent K_m was 272.2 ± 80.1 μmol/L (n = 3, ± SEM). The reaction was also dependent on NADPH and inhibitable by diphenyleneiodonium (10 μmol/L), indicating a requirement for the flavin cofactors in cytochrome *P*450 reductase (data not shown; Fig. 3B). In the presence of MMC (100 μmol/L), the V_{max} for NADPH use for H_2O_2 generation by cytochrome *P*450 reductase was increased by ~9-fold with no major changes in K_m (Table 2).

Table 2. Effects of MMC on kinetic constants for NADPH using recombinant cytochrome *P*450 reductase and microsome-containing fractions from different cell types

Species		Treatments	K_m (μmol/L)*	V_{max} (nmol H_2O_2/min/mg protein)
	CY *P*450 OR	–	28 ± 6	7.8 ± 1.3
		+ MMC	20 ± 7	70.8 ± 17.5
Hamster	CHO-WT	–	29 ± 8	0.2 ± 0.0
		+ MMC	17 ± 3	0.4 ± 0.0
	CHO-OR	–	31 ± 9	0.6 ± 0.1
		+ MMC	126 ± 20	16.4 ± 2.5
Mouse	MLE 15	–	19 ± 5	0.2 ± 0.0
		+ MMC	13 ± 2	1.2 ± 0.2
	RAW 264.7	–	20 ± 3	0.1 ± 0.0
		+ MMC	11 ± 2	0.8 ± 0.1
	C2	–	14 ± 3	0.2 ± 0.0
		+ MMC	14 ± 1	0.6 ± 0.0
	S 180	–	7 ± 1	0.2 ± 0.0
		+ MMC	10 ± 0	0.8 ± 0.0
	B16	–	28 ± 5	0.4 ± 0.1
		+ MMC	19 ± 5	0.9 ± 0.0
Human	HL-60	–	8 ± 2	0.1 ± 0.0
		+ MMC	7 ± 0	0.4 ± 0.0
	HT-29	–	ND†	ND
		+ MMC	3 ± 0	0.6 ± 0.0
	HeLa	–	8 ± 2	0.2 ± 0.0
		+ MMC	9 ± 1	0.9 ± 0.0
	PC-3	–	4 ± 1	0.1 ± 0.0
		+ MMC	8 ± 0	0.4 ± 0.0

*Using increasing concentrations of NADPH, reaction rates were measured in the linear phase in the absence and presence of MMC (100 μmol/L). K_m and V_{max} values were obtained using the Michaelis-Menton kinetics. In cell lysates, each point represents the mean of three independent determinations ± SEM. With CYP 450 OR, each point represents the mean of two independent determinations ± SD.

†Not determined (the data obtained do not fit the Michaelis-Menton kinetics).

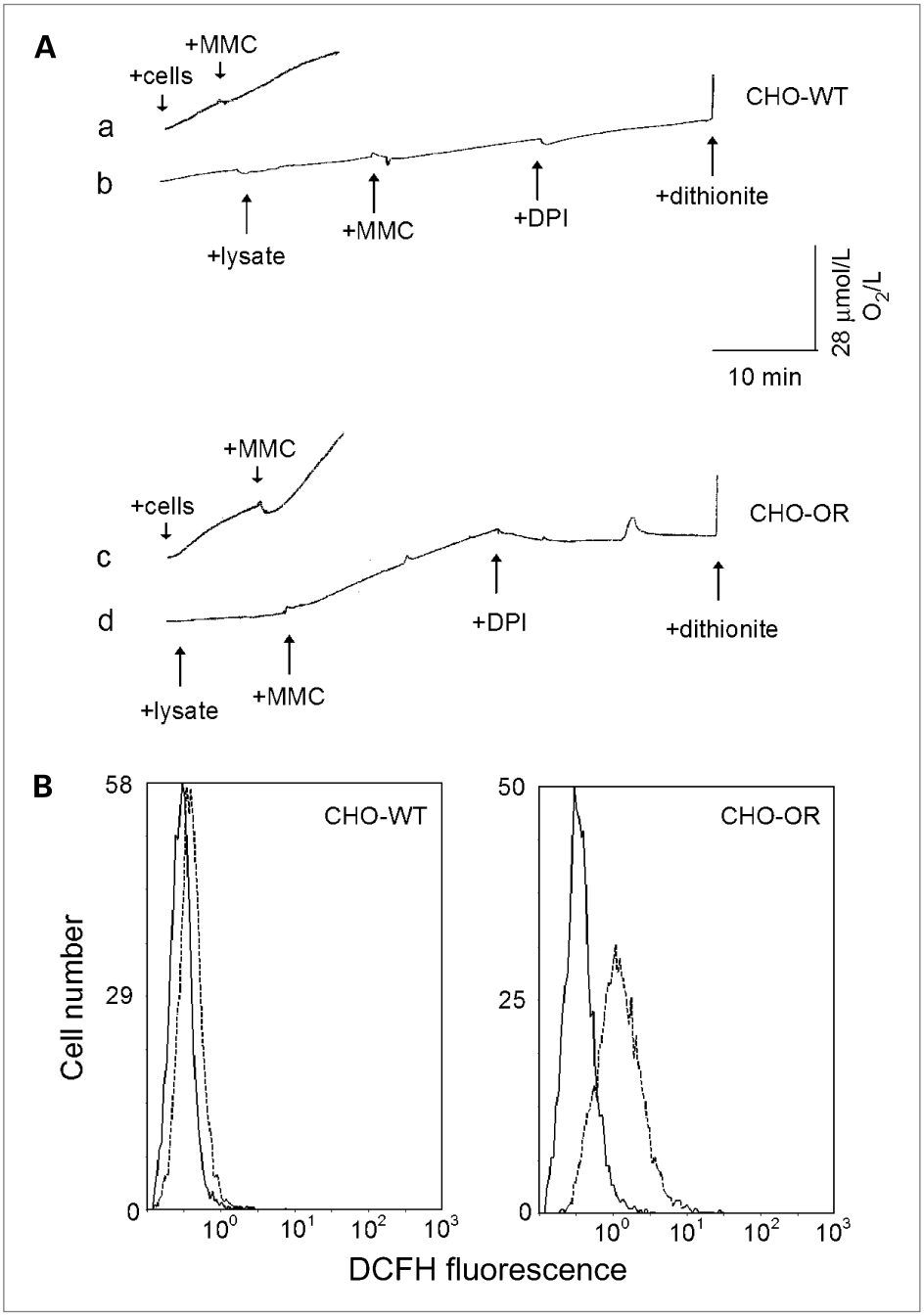

Figure 4. MMC-induced oxygen consumption and intracellular ROS production in CHO cells. A, stimulation of oxygen consumption in CHO-WT and CHO-OR cells by MMC. A Clark oxygen electrode was used to measure oxygen use in CHO cell lysates (tracings b and d) and intact CHO cells (tracings a and c). Arrows, the addition of lysates or cells, 0.5 mmol/L MMC, 10 µmol/L diphenyleneiodonium, and several grains of sodium dithionite. B, ROS production in intact CHO-WT and CHO-OR cells. DCFH-DA was used to quantify intracellular ROS generation. Cells were incubated with 5 µmol/L DCFH-DA at 37°C for 15 min and then incubated in the absence (solid lines) or presence (dashed lines) of 0.5 mmol/L MMC. After 3 h, cellular fluorescence was analyzed by flow cytometry. One representative experiment is shown. The mean fluorescence of the CHO-WT control peak was 0.32 ± 0.01 (mean ± SEM, $n = 3$) and 0.43 ± 0.03 after MMC treatment. For CHO-OR cells, the mean fluorescence of the control peak was 0.39 ± 0.00 and 1.50 ± 0.09 after MMC treatment.

We next compared the cytotoxicity of MMC in CHO-WT cells and CHO-OR cells. Surprisingly, overexpression of cytochrome *P*450 reductase had no effect on the sensitivity of the cells to MMC after 3 hours of incubation (IC_{50} = 2.5 µmol/L for CHO-WT cells and 3 µmol/L for CHO-OR cells) or 4 days of incubation (IC_{50} = 72 nmol/L for CHO-WT cells and 75 nmol/L for CHO-OR cells; Table 1; Fig. 1B), or its ability to arrest cells in the G_2-M and S phases of the cell cycle (Fig. 2A and B). This is in contrast to menadione, a quinone known to effectively redox cycle (30), which was found to be more cytotoxic in CHO-OR cells when compared with CHO-WT cells (Fig. 1C). In CHO-WT and CHO-OR cells, the effects of MMC were concentration dependent in the range of 0.003 to 3 µmol/L. Maximal cell cycle arrest was evident at the highest concentration of MMC.

In further studies, we characterized redox cycling in lysates of CHO-WT and CHO-OR cells. In the absence of MMC, low constitutive levels of H_2O_2 were generated by both cell types. Constitutive H_2O_2 levels were 2- to

3-fold greater in CHO-OR cells when compared with CHO-WT cells (Fig. 3C and D). The addition of MMC to the lysates resulted in a time- and concentration-dependent increase in H_2O_2 production in both cell types. Markedly greater maximal activity was detected in cells overexpressing cytochrome *P*450 reductase. The V_{max} for these cells was ~27-fold greater than for wild-type (WT) cells (32.4 nmol H_2O_2/min/mg protein versus 1.2 nmol H_2O_2/min/mg protein, respectively), whereas the K_m values for MMC in CHO-OR cells was ~2.5-fold greater than in CHO-WT cells (Table 1). MMC-stimulated H_2O_2 production was also associated with the increased metabolism of NADPH in CHO-WT and CHO-OR cells (data not shown; Table 2). In the presence of 100 μmol/L MMC, the K_m for NADPH increased 4-fold in CHO-OR cells with no major changes in the K_m for NADPH in CHO-WT cells. The V_{max} for NADPH for H_2O_2 generation also increased 27-fold in CHO-OR cells and only 2-fold in CHO-WT cells (Table 2).

MMC was also more effective in stimulating superoxide anion and hydroxyl radical production by lysates of CHO-OR cells when compared with CHO-WT cells. As observed with H_2O_2, low constitutive amounts of superoxide anion and hydroxyl radicals were generated in both cell types. Whereas significant increases in the production of superoxide anion were detected in lysates from CHO-OR cells treated with MMC, no significant effects were noted in CHO-WT cells (Fig. 3E). In CHO-OR cell lysates, superoxide anion production was readily inhibited by superoxide dismutase (Fig. 3E). Approximately two to four times greater quantities of hydroxyl radicals were produced by CHO-OR cells when compared with CHO-WT cells when treated with MMC (Fig. 3F). Hydroxyl radical formation was dependent on iron, and inhibited by catalase and DMSO (Fig. 3F).

To confirm these findings in intact cells, we used techniques in flow cytometry in conjunction with the ROS-sensitive probe, DCFH-DA. Consistent with our findings using Amplex-Red in cell lysates, MMC was found to cause a 4-fold increase in H_2O_2 production in intact CHO-OR cells ($P = 0.002$; Fig. 4B, right); in contrast, relatively small effects were observed in CHO-WT cells (1.4-fold, $P = 0.01$; Fig. 4B, left).

Effects of MMC on oxygen consumption

Using mitochondria-free lysates, we observed that oxygen use was maintained at low levels in both CHO cell types. The addition of 0.5 mmol/L MMC stimulated oxygen consumption in lysates of CHO-OR, but not CHO-WT cells (Fig. 4A, tracings b and d). Increased oxygen use in CHO-OR cells was inhibited by diphenyleneiodonium, a finding consistent with flavin-mediated MMC redox cycling by cytochrome *P*450 reductase (8, 11). We also found that MMC caused marked increases in oxygen consumption in intact CHO-OR cells, but not in intact CHO-WT cells (Fig. 4A, tracings a and c).

Effects of MMC on redox cycling and cytotoxicity in tumor cell lines varying in cytochrome *P*450 reductase activity

We next compared MMC redox cycling and cytotoxicity in nine different mouse and human tumor cell lines that varied in cytochrome *P*450 reductase activity (27). MMC redox cycling was detectable in lysates from each of these tumor cell types. The greatest activity, as measured by H_2O_2 production, was observed in mouse MLE 15 cells, whereas human PC-3 and HL-60 cells and hamster CHO-WT cells contained the lowest activity. The apparent K_m for MMC was also greatest in MLE 15 cells (Table 1). As observed with recombinant cytochrome *P*450 reductase, MMC (100 μmol/L) increased the V_{max} for NADPH for H_2O_2 generation in the cell lines with no major changes in the K_m values (Table 2). In the tumor cell lines, a strong correlation ($r^2 = 0.996$ including CHO-OR cells in the analysis and $r^2 = 0.929$ without CHO-OR cells in the analysis) was observed between MMC-induced H_2O_2 generation during redox cycling and cytochrome *P*450 reductase activity (Fig. 2C, left). However, as observed with CHO-WT and CHO-OR cells, MMC-induced cytochrome *P*450 reductase activity and MMC redox cycling were not associated with cytotoxicity in the different tumor cell lines (Fig. 2C, right).

Effects of hypoxia on cytotoxicity of MMC

Several laboratories have suggested that the reaction of cells with MMC under hypoxic conditions increases its cytotoxicity due to the stabilization of the highly reactive semiquinone free radical intermediate (31, 32). Interestingly, we found that exposure of CHO-WT and CHO-OR cells to MMC under hypoxic conditions for either 3 or 24 hours had no effect on their sensitivity to MMC (Table 1; Fig. 1B). This is in contrast to menadione, in which increased cytotoxicity was observed in CHO-OR cells under hypoxic conditions (Fig. 1C). Moreover, despite marked differences in the ability of the nine tumor cell lines to redox cycle MMC, hypoxia caused no significant alterations in their sensitivity to the drug (Table 1).

Discussion

NADPH-dependent one-electron reduction of MMC and subsequent generation of ROS have been shown using reconstituted microsomal systems, purified cytochrome *P*450 reductase from rat liver (8, 11), and human recombinant enzyme (3). The present studies show that the rat recombinant enzyme is also highly effective in MMC redox cycling. Moreover, kinetic parameters for the recombinant enzyme, with respect to the generation of H_2O_2, were generally similar to the previous reports using purified rat cytochrome *P*450 reductase (11). MMC redox cycling initiated by the recombinant enzyme was due to an increase in the V_{max} for NADPH for H_2O_2 generation with little or no change in affinity of the enzyme for the pyridine nucleotide. To further

investigate the role of cytochrome *P*450 reductase in MMC-induced redox cycling, we analyzed this process in CHO WT cells and CHO cells overexpressing cytochrome *P*450 reductase, and in different mouse and human tumor cell lines varying in cytochrome *P*450 reductase content. Redox cycling of MMC was evident in all cell types, although none was as efficient as recombinant rat cytochrome *P*450 reductase in generating ROS. This is likely due to the dilution of the reductase in tumor cell lysates and the competition from other enzymes that either mediate redox cycling and/or detoxify ROS (9, 10, 29). The K_ms and V_{max}s for MMC redox cycling in most of the cell lines were generally in the same concentration range with the exception of CHO-OR cells. The higher V_{max} in these cells can be attributed to the greater expression of cytochrome *P*450 reductase. MMC metabolism in all tumor cells assayed increased the V_{max} for NADPH for H_2O_2 generation; no major changes in the enzyme affinity for NADPH except in CHO-OR cells were noted. As observed with redox cycling, the kinetic parameters for NADPH for H_2O_2 generation in the different cell lines represent the specific characteristics of the enzyme activities mediating the one-electron reduction of MMC. The mechanisms underlying the distinct reaction kinetics for NADPH in CHO-OR cells are not readily apparent, and it will be of interest to further characterize the enzymes that are important in MMC metabolism in this and other cell lines.

In addition to generating H_2O_2 during MMC redox cycling, cell lysates from CHO-OR cells produced superoxide anion and, in the presence of redox active iron, hydroxyl radicals. As expected, this was associated with increased oxygen consumption due to the rapid reaction of the MMC semiquinone radical with molecular oxygen. MMC was also found to be active in redox cycling in intact CHO-OR cells, as evidenced by increased H_2O_2 formation and oxygen consumption. Both the generation of ROS and increased oxygen use can contribute to cellular oxidative stress (33).

MMC was also found to be a potent growth inhibitor for CHO cells. Despite marked differences in cytochrome *P*450 reductase content and redox cycling in CHO-WT and CHO-OR cells, no significant differences were noted between the cell types in their sensitivity to the growth-inhibitory actions of MMC or its ability to arrest cells in the G_2-M and S phases of the cell cycle. These unexpected findings prompted us to compare cytochrome *P*450 reductase activity, redox cycling, and sensitivity to MMC in other tumor cell types varying in cytochrome *P*450 reductase. Indeed, despite a direct correlation between cytochrome *P*450 reductase activity and redox cycling in nine different mouse and human tumor cell lines, there was no correlation between redox cycling and growth inhibition. These data are consistent with those from Fitzsimmons and colleagues (17), who compared the activities of cytochrome *P*450 reductase, cytochrome b5 reductase, and DT-diaphorase, and the cytotoxicity of MMC and a related indolequinone 3-hydroxy-5-aziridinyl-1-methyl-2[indole-4,7-dione]-prop-β-en-(-ol) (EO9) in 69 NCI tumor cell lines. In these studies, the sensitivity of the cells to MMC and EO9 correlated with DT-diaphorase, which mediates the two-electron reduction of MMC, but not with cytochrome *P*450 reductase and cytochrome b5 reductase, which mediate redox cycling. Several other laboratories have similarly described a correlation between DT-diaphorase expression and sensitivity to MMC or related indoloquinones in different tumor cell lines, breast tumor xenographs, and DT-diaphorase overexpressing cells (15, 34, 35). Resistance to MMC has also been correlated with reduced DT-diaphorase activity (36).

In contrast to our studies, a direct correlation between the expression of cytochrome *P*450 reductase and sensitivity to MMC has been described in cell lines and tumor tissue by several laboratories. This includes breast tumor cells in culture and maintained as xenographs (15, 16), as well as variant CHO cell lines overexpressing cytochrome *P*450 reductase (13, 14). Differences between our findings and previous reports using CHO cells, with respect to sensitivity to MMC and cytochrome *P*450 reductase expression, may be due to methods used to assess cytotoxicity. Although our growth inhibition assays showed no differences in MMC sensitivity between CHO-WT and CHO-OR cells following either a 3-hour or a 4-day exposure, Belcourt et al. (13) and Seow et al. (14) reported increased sensitivity of their cytochrome *P*450 reductase–overexpressing CHO cells when treated with MMC for 1 hour. One can speculate that the sensitivity of the different cells to MMC may be due to differences in uptake and/or metabolism of the drug during the exposure. Belcourt et al. (13) and Seow et al. (14) also used clonogenic assays to assess cytotoxicity and it may be that this assay selects for cells with altered sensitivity to the drug. Selected clones may express other enzymes reported to activate MMC such as DT-diaphorase (17, 35), NRH:quinone oxidoreductase 2 (37, 38), NADPH-ferrodoxin reductase (39), or cytochrome b5 reductase (9); they may also express antioxidants that detoxify and protect against ROS-induced damage. In this regard, antioxidant enzymes including glutathione peroxidase, superoxide dismutase, and catalase have all been shown to reduce or abolish MMC cytotoxicity in tumor cells *in vitro* (29, 40).

It is well recognized that hypoxia can enhance the biological activity of redox-active chemotherapeutic agents, presumably through the stabilization of the one-electron reduced drug (32). In the case of MMC, this is the highly reactive MMC semiquinone radical (Fig. 1A; ref. 32). Under hypoxic conditions, the MMC semiquinone radical can also rearrange to form the more stable hydroquinone (5, 7). Increased cytotoxicity of MMC under hypoxic conditions has been reported previously. For example, Keyes et al. (41) found that hypoxia enhanced the sensitivity of EMT6 mouse breast carcinoma cells and V79 Chinese hamster lung fibroblasts to MMC. Belcourt and colleagues (13, 42) and Seow and colleagues (14) reported that MMC

was more cytotoxic in CHO cells overexpressing cytochrome *P*450 reductase under hypoxic conditions. Interestingly, these investigators found little or no difference in the cytotoxicity of MMC in parental CHO cells under hypoxic and aerobic conditions, despite the fact that these cells readily redox cycle MMC. In contrast, in our studies, we found no differences in the cytotoxicity of MMC under hypoxic conditions in CHO-WT or CHO-OR cells, or in the different tumor cell lines that varied in cytochrome *P*450 reductase activity. Each cell type can mediate the one-electron reduction of MMC and it is presumed that this process occurs in the cells under hypoxic conditions. If semiquinone radicals are in fact stabilized in cells under hypoxia, they do not seem to mediate MMC-induced growth inhibition. Our results are in accord with earlier studies showing no significant differences in cytotoxicity of MMC or the related analogue EO9 under aerobic and hypoxic conditions in A2780 human ovarian tumor cells or HT-29 colon tumor cells (43–45).

The precise mechanisms mediating the distinct sensitivities of the different tumor cell lines to MMC under aerobic and hypoxic conditions are not known. One- and two-electron reduction of MMC occurs in the presence and absence of oxygen, and electrophilic intermediates formed as a result are active alkylating species that can modify DNA-forming monoadducts, intrastrand cross-links, and DNA-DNA interstrand cross-links (46). The relative formation of the different reduced species of MMC at different oxygen tensions and their contribution to toxicity in each cell line have not been determined. In the presence of oxygen, MMC redox cycling generates ROS that can contribute to the biological effects of MMC. Whether or not ROS contribute to the actions of MMC may depend, as indicated above, not only on antioxidant enzymes (29, 40), but also small-molecular-weight antioxidants such as glutathione, α-tocopherol, and ascorbic acid, which can detoxify oxidants. However, it is important to note that MMC-induced ROS formation does not seem to directly mediate cytotoxicity as evidenced by the fact that no correlation was observed between the capacity of the different cells to generate ROS and cell growth inhibition. Our previous work showing that cytochrome *P*450 reductase activity and ROS generation by nitrofurantoin redox cycling do not correlate with cell growth inhibition in the tumor cell lines suggests that the present findings are not specific for MMC (27). In this regard, Ramji and colleagues (47) have shown that redox cycling of doxorubicin is also not correlated with cytotoxicity in cytochrome *P*450 reductase–overexpressing breast cancer cell lines. It has previously been reported that MMC-induced cytotoxicity is correlated with the activity of enzymes mediating its two-electron reduction (15, 17, 34, 35). This suggests that the MMC hydroquinone intermediate may be important in growth inhibition observed in our studies including CHO-OR cells, which are highly efficient in generating ROS. This is supported by our findings that hypoxia has no effect on MMC-induced cytotoxicity. Other enzymes in CHO-OR cells that can mediate the two-electron reduction of MMC include NRH:quinone oxidoreductase 2 (37, 38). We also cannot exclude the possibility that other enzymes mediating the one-electron reduction of MMC including NADH-cytochrome b5 reductase, xanthine oxidase, and nitric oxide synthase also mediate cytotoxicity in these cells. Further studies are needed to more precisely characterize the metabolism of MMC under aerobic and hypoxic conditions to identify the enzymes mediating this process and to better define MMC-induced growth-limiting events in the different tumor cell lines.

Disclosure of Potential Conflicts of Interest

No potential conflicts of interest were disclosed.

Grant Support

NIH grants CA100994 (J.D. Laskin), CA093798 (D.E. Heck), ES005022 (J.D. Laskin and D.L. Laskin), ES004738 (D.L. Laskin and J.D. Laskin), CA132624 (D.L. Laskin and J.D. Laskin), AR055073 (J.D. Laskin, D.L. Laskin, and D.E. Heck), and GM034310 (D.L. Laskin and J.D. Laskin; and funded in part by the NIH CounterACT Program through the National Institute of Arthritis and Musculoskeletal and Skin Diseases award no. U54AR055073 (J.D. Laskin). Its contents are solely the responsibility of the authors and do not necessarily represent the official views of the federal government.

The costs of publication of this article were defrayed in part by the payment of page charges. This article must therefore be hereby marked *advertisement* in accordance with 18 U.S.C. Section 1734 solely to indicate this fact.

Received 11/30/2009; revised 03/22/2010; accepted 03/30/2010; published OnlineFirst 05/25/2010.

References

1. Begleiter A. Clinical applications of quinone-containing alkylating agents. Front Biosci 2000;5:E153–71.
2. Belcourt MF, Penketh PG, Hodnick WF, et al. Mitomycin resistance in mammalian cells expressing the bacterial mitomycin C resistance protein MCRA. Proc Natl Acad Sci U S A 1999;96:10489–94.
3. Krishna MC, DeGraff W, Tamura S, et al. Mechanisms of hypoxic and aerobic cytotoxicity of mitomycin C in Chinese hamster V79 cells. Cancer Res 1991;51:6622–8.
4. Komiyama T, Kikuchi T, Sugiura Y. Generation of hydroxyl radical by anticancer quinone drugs, carbazilquinone, mitomycin C, aclacinomycin A and adriamycin, in the presence of NADPH-cytochrome P-450 reductase. Biochem Pharmacol 1982;31:3651–6.
5. Baumann RP, Hodnick WF, Seow HA, et al. Reversal of mitomycin C resistance by overexpression of bioreductive enzymes in Chinese hamster ovary cells. Cancer Res 2001;61:7770–6.
6. Butler J, Hoey BM, Swallow AJ. Reactions of the semiquinone free radicals of anti-tumour agents with oxygen and iron complexes. FEBS Lett 1985;182:95–8.
7. Hoey BM, Butler J, Swallow AJ. Reductive activation of mitomycin C. Biochemistry 1988;27:2608–14.
8. Bachur NR, Gordon SL, Gee MV, Kon H. NADPH cytochrome P-450 reductase activation of quinone anticancer agents to free radicals. Proc Natl Acad Sci U S A 1979;76:954–7.
9. Hodnick WF, Sartorelli AC. Reductive activation of mitomycin C by NADH:cytochrome b5 reductase. Cancer Res 1993;53:4907–12.

10. Pan SS, Andrews PA, Glover CJ, Bachur NR. Reductive activation of mitomycin C and mitomycin C metabolites catalyzed by NADPH-cytochrome P-450 reductase and xanthine oxidase. J Biol Chem 1984;259:959–66.
11. Vromans RM, van de Straat R, Groeneveld M, Vermeulen NP. One-electron reduction of mitomycin c by rat liver: role of cytochrome P-450 and NADPH-cytochrome P-450 reductase. Xenobiotica 1990;20:967–78.
12. Jiang HB, Ichikawa M, Furukawa A, Tomita S, Ichikawa Y. Reductive activation of mitomycin C by neuronal nitric oxide synthase. Biochem Pharmacol 2000;60:571–9.
13. Belcourt MF, Hodnick WF, Rockwell S, Sartorelli AC. Differential toxicity of mitomycin C and porfiromycin to aerobic and hypoxic Chinese hamster ovary cells overexpressing human NADPH: cytochrome *c* (P-450) reductase. Proc Natl Acad Sci U S A 1996;93: 456–60.
14. Seow HA, Belcourt MF, Penketh PG, et al. Nuclear localization of NADPH:cytochrome *c* (*P*450) reductase enhances the cytotoxicity of mitomycin C to Chinese hamster ovary cells. Mol Pharmacol 2005;67:417–23.
15. Cowen RL, Patterson AV, Telfer BA, et al. Viral delivery of *P*450 reductase recapitulates the ability of constitutive overexpression of reductase enzymes to potentiate the activity of mitomycin C in human breast cancer xenografts. Mol Cancer Ther 2003;2:901–9.
16. Martinez VG, Williams KJ, Stratford IJ, Clynes M, O'Connor R. Overexpression of cytochrome *P*450 NADPH reductase sensitises MDA 231 breast carcinoma cells to 5-fluorouracil: possible mechanisms involved. Toxicol In Vitro 2008;22:582–8.
17. Fitzsimmons SA, Workman P, Grever M, Paull K, Camalier R, Lewis AD. Reductase enzyme expression across the National Cancer Institute Tumor cell line panel: correlation with sensitivity to mitomycin C and EO9. J Natl Cancer Inst 1996;88:259–69.
18. Han JF, Wang SL, He XY, Liu CY, Hong JY. Effect of genetic variation on human cytochrome p450 reductase-mediated paraquat cytotoxicity. Toxicol Sci 2006;91:42–8.
19. Mariano TM, Vetrano AM, Gentile SL, et al. Cell-impermeant pyridinium derivatives of psoralens as inhibitors of keratinocyte growth. Biochem Pharmacol 2002;63:31–9.
20. Baumann RP, Penketh PG, Seow HA, Shyam K, Sartorelli AC. Generation of oxygen deficiency in cell culture using a two-enzyme system to evaluate agents targeting hypoxic tumor cells. Radiat Res 2008;170:651–60.
21. Wardman P, Dennis MF, Everett SA, Patel KB, Stratford MR, Tracy M. Radicals from one-electron reduction of nitro compounds, aromatic N-oxides and quinones: the kinetic basis for hypoxia-selective, bioreductive drugs. Biochem Soc Symp 1995;61:171–94.
22. Wardman P. Electron transfer and oxidative stress as key factors in the design of drugs selectively active in hypoxia. Curr Med Chem 2001;8:739–61.
23. Laskin DL, Beavis AJ, Sirak AA, O'Connell SM, Laskin JD. Differentiation of U-937 histiocytic lymphoma cells towards mature neutrophilic granulocytes by dibutyryl cyclic adenosine-3′,5′-monophosphate. Cancer Res 1990;50:20–5.
24. Zhou M, Diwu Z, Panchuk-Voloshina N, Haugland RP. A stable nonfluorescent derivative of resorufin for the fluorometric determination of trace hydrogen peroxide: applications in detecting the activity of phagocyte NADPH oxidase and other oxidases. Anal Biochem 1997; 253:162–8.
25. Mishin VM, Thomas PE. Characterization of hydroxyl radical formation by microsomal enzymes using a water-soluble trap, terephthalate. Biochem Pharmacol 2004;68:747–52.
26. Zhao H, Joseph J, Fales HM, et al. Detection and characterization of the product of hydroethidine and intracellular superoxide by HPLC and limitations of fluorescence. Proc Natl Acad Sci U S A 2005; 102:5727–32.
27. Wang Y, Gray JP, Mishin V, Heck DE, Laskin DL, Laskin JD. Role of cytochrome *P*450 reductase in nitrofurantoin-induced redox cycling and cytotoxicity. Free Radic Biol Med 2008;44:1169–79.
28. Heck DE, Laskin DL, Gardner CR, Laskin JD. Epidermal growth factor suppresses nitric oxide and hydrogen peroxide production by keratinocytes. Potential role for nitric oxide in the regulation of wound healing. J Biol Chem 1992;267:21277–80.
29. Doroshow JH. Role of hydrogen peroxide and hydroxyl radical formation in the killing of Ehrlich tumor cells by anticancer quinones. Proc Natl Acad Sci U S A 1986;83:4514–8.
30. Smith PF, Alberts DW, Rush GF. Role of glutathione reductase during menadione-induced NADPH oxidation in isolated rat hepatocytes. Biochem Pharmacol 1987;36:3879–84.
31. Cummings J, Spanswick VJ, Tomasz M, Smyth JF. Enzymology of mitomycin C metabolic activation in tumour tissue: implications for enzyme-directed bioreductive drug development. Biochem Pharmacol 1998;56:405–14.
32. Seow HA, Penketh PG, Baumann RP, Sartorelli AC. Bioactivation and resistance to mitomycin C. Method Enzymol 2004;382:221–33.
33. Neuzil J, Gebicki JM, Stocker R. Radical-induced chain oxidation of proteins and its inhibition by chain-breaking antioxidants. Biochem J 1993;293:601–6.
34. Belcourt MF, Hodnick WF, Rockwell S, Sartorelli AC. Bioactivation of mitomycin antibiotics by aerobic and hypoxic Chinese hamster ovary cells overexpressing DT-diaphorase. Biochem Pharmacol 1996;51: 1669–78.
35. Mikami K, Naito M, Tomida A, Yamada M, Sirakusa T, Tsuruo T. DT-diaphorase as a critical determinant of sensitivity to mitomycin C in human colon and gastric carcinoma cell lines. Cancer Res 1996;56:2823–6.
36. Yoshida T, Tsuda H. Gene targeting of DT-diaphorase in mouse embryonic stem cells: establishment of null mutant and its mitomycin C-resistance. Biochem Biophys Res Commun 1995;214:701–8.
37. Celli CM, Tran N, Knox R, Jaiswal AK. NRH:quinone oxidoreductase 2 (NQO2) catalyzes metabolic activation of quinones and anti-tumor drugs. Biochem Pharmacol 2006;72:366–76.
38. Jamieson D, Tung AT, Knox RJ, Boddy AV. Reduction of mitomycin C is catalysed by human recombinant NRH:quinone oxidoreductase 2 using reduced nicotinamide adenine dinucleotide as an electron donating co-factor. Brit J Cancer 2006;95:1229–33.
39. Jiang HB, Ichikawa M, Furukawa A, Tomita S, Ohnishi T, Ichikawa Y. Metabolic activation of mitomycin C by NADPH-ferredoxin reductase *in vitro*. Life Sci 2001;68:1677–85.
40. Doroshow JH, Akman S, Esworthy S, Chu FF, Burke T. Doxorubicin resistance conferred by selective enhancement of intracellular glutathione peroxidase or superoxide dismutase content in human MCF-7 breast cancer cells. Free Radic Res Commun 1991;12-13 Pt 2:779–81.
41. Keyes SR, Fracasso PM, Heimbrook DC, Rockwell S, Sligar SG, Sartorelli AC. Role of NADPH:cytochrome *c* reductase and DT-diaphorase in the biotransformation of mitomycin C1. Cancer Res 1984;44:5638–43.
42. Belcourt MF, Hodnick WF, Rockwell S, Sartorelli AC. Exploring the mechanistic aspects of mitomycin antibiotic bioactivation in Chinese hamster ovary cells overexpressing NADPH:cytochrome C (P-450) reductase and DT-diaphorase. Adv Enzyme Regul 1998;38:111–33.
43. Samuni AM, DeGraff W, Krishna MC, Mitchell JB. Nitroxides as antioxidants: Tempol protects against EO9 cytotoxicity. Mol Cell Biochem 2002;234-5:327–33.
44. O'Dwyer PJ, Perez RP, Yao KS, Godwin AK, Hamilton TC. Increased DT-diaphorase expression and cross-resistance to mitomycin C in a series of cisplatin-resistant human ovarian cancer cell lines. Biochem Pharmacol 1996;52:21–7.
45. Beall HD, Mulcahy RT, Siegel D, Traver RD, Gibson NW, Ross D. Metabolism of bioreductive antitumor compounds by purified rat and human DT-diaphorases. Cancer Res 1994;54:3196–201.
46. Iyer VN, Szybalski W. A molecular mechanism of mitomycin action: linking of complementary DNA strands. Proc Natl Acad Sci U S A 1963;50:355–62.
47. Ramji S, Lee C, Inaba T, Patterson AV, Riddick DS. Human NADPH-cytochrome p450 reductase overexpression does not enhance the aerobic cytotoxicity of doxorubicin in human breast cancer cell lines. Cancer Res 2003;63:6914–9.